



ERD. 980909.0004

Water Resources Center

August 31, 1998

Monica Sanchez
Environmental Restoration Division
Nevada Operations Office
U.S. Department of Energy
P.O. Box 98518
Las Vegas, NV 89193-8518

Dear Ms. Sanchez:

Enclosed with this letter is a report prepared to support the modeling approach that we recommend for Amchitka Island. The report attempts to explain the differences between the Amchitka modeling and other modeling efforts that do not need to consider the effects of density-coupled flow. As you will see, the recommendations do not come to the simple point of deciding between 2-D and 3-D approaches. A number of complicating factors (e.g., presence of faults) do require an expanded 3-D effort, but should not drive all of the modeling in that direction. In summary, we believe that a modeling approach that simultaneously considers the various parameters at the island would be extremely computationally expensive. This expense is not likely to be justified when the limited amount of available hydraulic data is considered.

In response, we have proposed a modeling effort that investigates the possible effects of various parameters (e.g., heat-dependent buoyancy) on an individual basis. The individual studies will be conducted using the simplest, most efficient means available. If a steady-state flow field under the island is judged to be a reasonable assumption following these studies, then the most important parameters will be incorporated into a final flow model for each test. One or more streamtubes from each flow model will be extracted and discretized in a radionuclide transport simulation that incorporates matrix diffusion. The statistics of the generated breakthrough curves, as well as position of seepage into the ocean, will be the result of the study.

If a steady-state approach is not reasonable (if, for example, flow driven by heat from the tests is likely), then the scope of the modeling effort increases substantially. Recommendations for the additional work would be delivered along with the results to that point.

If you have any questions concerning the attached decision-support paper, please call me at 895-0459, or David Benson (in Reno) at 673-7496.

Sincerely,

Jenny Chapman
Associate Research Hydrogeologist

cc w/encl: Frank Maxwell, DOE
:2571

P.O. Box 60220
Reno, NV 89506-0220
702-673-7361
Fax 702-673-7397

ACTION	_____
INFO	_____ <i>ERD</i>
MGR	_____
AMBFS	_____
AMTS	_____
AMNS	_____
AMEM	_____



AMC 530.02

INTRODUCTION

This decision-support paper summarizes the proposed conceptual plan for numerical modeling of radionuclide transport at Amchitka Island, in Alaska's Aleutian chain. It is based on:

- A review of geologic and hydrologic data previously reported for the island;
- Previous conceptual and numerical models of the flow system beneath the island;
- A review of readily available numerical codes capable of simulating one or more of the physical processes that are potentially present in the island's flow and transport system; and
- Preliminary (scoping-level) simulations to assess implementation of several readily available codes.

This document does not contain exhaustive information concerning the hydrogeology of the island or the fate and transport of radionuclides. Rather, it supports the proposed modeling effort, including hydrologic data assimilation and analysis. It includes a review of the current understanding of the hydrogeology of islands in general, and Amchitka Island in particular, to aid in the identification and prioritization of the probable mechanisms that influence radionuclide migration to the biosphere via groundwater movement.

The radionuclides generated by the three underground nuclear tests on Amchitka Island only pose a threat if individuals can be exposed to those contaminants through some environmental pathway. The hydrogeology of Amchitka Island and the emplacement of the nuclear tests dictate that the only probable exposure pathway to humans is by dissolution of radionuclides in groundwater, migration with the groundwater, and discharge from the subsurface into the marine environment. Exposure is projected to occur as a result of migration of radionuclides through the food chain, ultimately to human receptors. The current absence of groundwater use on the island is assumed to continue so that no pumping scenarios are considered. The data needed for the risk assessment are the concentration (mean and variance) of radionuclides that discharge into the ocean, as well as knowledge of where on the seafloor the discharge occurs so that appropriate food webs can be constructed. From that point, the hydrogeologic pathway is complete and the risk assessment turns to issues of dilution in the ocean and incorporation of the dissolved contaminants into the food chain. This hydrogeologic pathway, however, is through a complex system affected by processes that require state-of-the-art modeling approaches. The modeling approach, and details of the system that dictate it, are the topic of the discussion presented below.

Purpose

The purpose of the numerical modeling of Amchitka Island is to predict radionuclide mass flux (or concentration) across the seepage face into the ocean from each of the three nuclear tests. Included in this purpose is the prediction of the location of the areas of ocean bottom across which the radionuclides will travel.

Review of Island Hydrogeology

A brief review of the hydrogeologic characteristics shared by all islands is required to understand the work that must be undertaken to predict radionuclide migration at Amchitka. A more thorough review is given by Wheatcraft (1995).

Since the density of seawater is approximately 4 percent greater than freshwater, any rainwater that infiltrates an island's ground surface collects in a buoyant lens. As this lens, or mound, grows thicker, the freshwater head at the center of the island exceeds the head at the edge of the island, resulting in flow of freshwater from the island center toward the ocean. Like an iceberg, the majority of the freshwater lens, including the portion that seeps into the ocean, exists at elevations lower than sea level (Figure 1). The freshwater lens reaches a relatively steady state wherein the net recharge to the island balances the seepage into the ocean. The thickness of the lens is ultimately related to the effective (island-wide average) permeability (k), the amount of recharge, and the land surface elevation. Lower values of permeability restrict the flux of water toward the ocean, resulting in a buildup of freshwater and a thicker lens. If the land surface is at an elevation lower than the steady-state water table elevation for a given value of k , then infiltration is limited and precipitation is routed to surface runoff.

Freshwater that accumulates directly atop the seawater does not remain pristine. Diffusion of salt creates a transition zone of varying thickness. Any salt that migrates into the moving freshwater will ultimately discharge into the ocean. Since salt mass must be conserved in the subsurface, this salt must be replaced. Seawater crosses the ocean bottom to replace the salt, and a flow system is set into motion within the saltwater that underlies the freshwater lens. Saltwater enters the system farther asea, since the seawater that is partially stripped of salt at the transition zone must exit the system near shore. This water will now lose more salt, since the moving seawater will experience hydrodynamic dispersion, which is much more effective at mixing water than molecular diffusion alone. The hydrodynamic dispersion enlarges the transition zone (increasing salt flux) until an equilibrium is reached between the velocity-dependent dispersion, the salt flux, and the volume of seawater needed to recharge the system with salt.

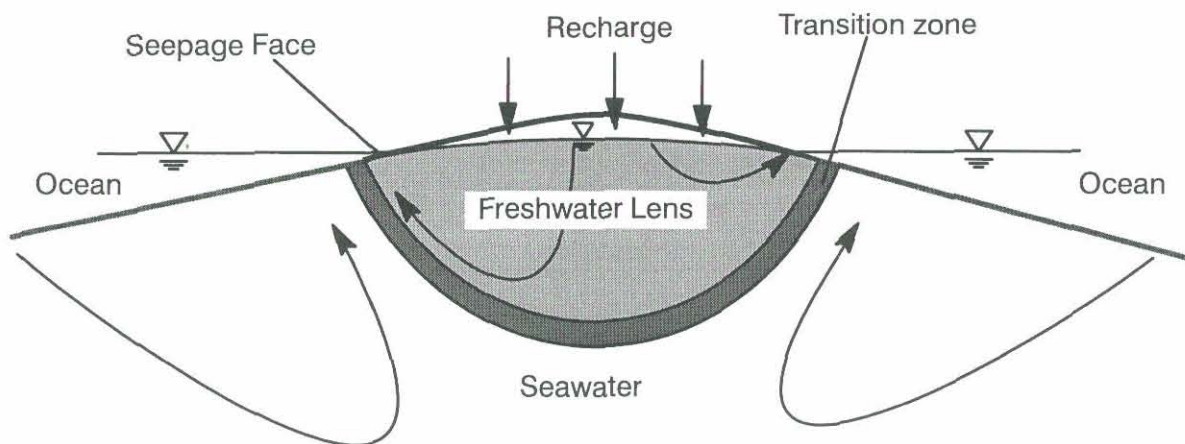


Figure 1. Salt water intrusion beneath island aquifers. Typical flowpaths are indicated by the curved arrows.

Several factors naturally complicate and accentuate this process. Tides change the seawater head and temporarily alter the “equilibrium” interface position. The daily tidal fluctuations are thought to enlarge the transition zone through continuous up and down motion of the mixing zone. This increases the total salt flux, and thereby increases the velocity within all of the seawater recirculation zone. A similar effect would be anticipated for temporally variable recharge.

In contrast to typical groundwater flow systems that have a single density fluid, the velocity is highly variable in space under an island, even if k is completely homogeneous. The velocity variability is due to the contorted nature of the freshwater and saltwater flow fields (Figure 1). This peculiarity indicates that a number of physical phenomena that are typically considered negligible in terrestrial studies must be considered in this study. For example, if recharge variability doubles the width of the transition zone, do the velocities in the saltwater well below the transition zone essentially double? Further, since velocity is highly variable in relation to distance from the transition zone, it is important to accurately estimate the elevation of the transition zone at the nuclear test points. The various parameters and measurements are discussed later in this document.

Another interesting feature of the island recharge/seawater intrusion problem is the ultimate discharge point of both freshwater and saline water. The freshwater moves toward the relatively shallow (nearshore) seepage face. The saltwater circulation dictates that the discharge point for deep seawater (or seawater near the recharge axis of the island) and saline water near the transition zone is also near the seepage face (Figure 1). Even for a range of system parameters, the discharge point for most water beneath the land surface of the island is close to shore (typically within several kilometers).

The driving force that creates the dynamic lens system is the movement of freshwater that results from the difference in head between the freshwater mound and sea level. In the case of a roughly circular island, the predominant flow direction would be radially outward. In the case of a long, thin island such as Amchitka, the predominant horizontal component of the flow direction is expected to be perpendicular to the long axis of the island. Major discontinuities in the permeability field, such as those created by faults, may subtly alter the flow field.

HYDROGEOLOGY OF AMCHITKA ISLAND

Amchitka Island (Figure 2) is located approximately two-thirds of the way out the Aleutian Island chain. Since the Aleutians are an island arc associated with a convergent plate boundary, the rocks that underlie the island are primarily volcanic in origin. Exceptions to this rule are intrusive bodies (dikes, sills, and stocks) and clastic sedimentary rocks (sand- and siltstones) of submarine deposition. The volcanic rock is primarily basaltic to andesitic breccia and pillow lava indicating shallow underground to submarine deposition (Carr *et al.*, 1966). Several of the rock types that indicate different depositional environment generally correlate between drillholes across the island. The majority of the rock is breccia, with sand- to gravel-sized basaltic lithic fragments. The breccia shows various degrees of cementation and vitrification. The breccias, basalts and andesites all exhibit evidence of fracturing on geophysical logs. When recorded on logs, the orientation of the fracturing is dominantly steeply-dipping ($>70^\circ$). Also reported are infrequent beds of sorted sandstone and siltstone that indicate submarine erosion and deposition. These beds are

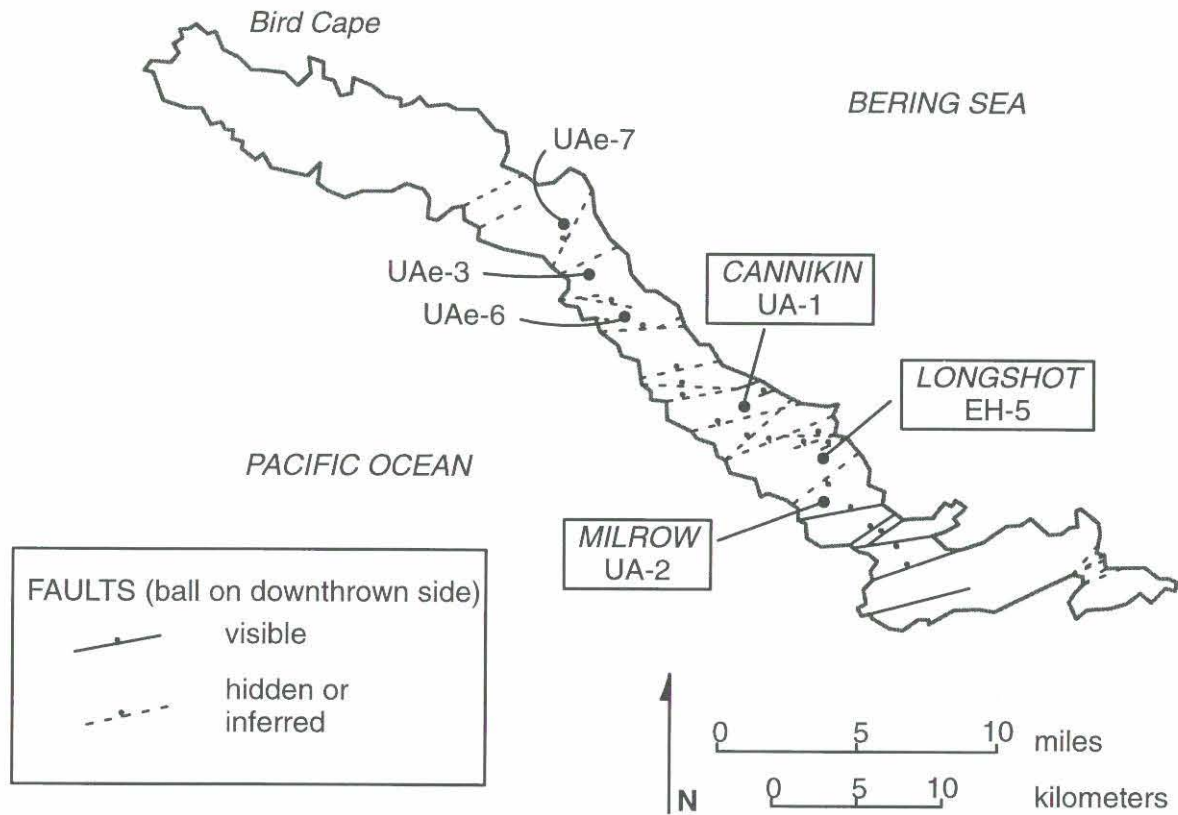


Figure 2. Test well and fault locations on Amchitka Island. Base map from von Huene *et al.* (1971).

hydrologically inconsequential due to their percentage of the rock column and probable similarity of hydraulic properties to the surrounding fractured breccia.

The island is reportedly traversed by numerous faults. A number of the faults were mapped by locating lineation features or oceanic embayment on aerial photographs (Carr *et al.*, 1966). Air and shipborne magnetometer and seismic surveys were also used to locate a number of faults (von Huene *et al.*, 1971). Fewer faults were mapped by visible evidence of offset. Most of the faults have a strike in the ENE direction, which is nearly parallel with the minor axis of the island (Figure 2). A secondary direction is roughly due East. It is unknown whether movement along these faults has tended to increase or decrease the permeability of the rocks they transect, although Carr *et al.* (1966) report that the major fault zones are relatively wide (up to thousands of feet) and composed of highly fractured rock. In any case, the presence of the faults will slightly alter the flowpaths that groundwater will take when moving from beneath the island toward the ocean.

A number of test and emplacement holes were drilled near the long axis of the island, allowing the construction of a vertical geologic section (Figure 3). Several important hydrologic features are shown in the section. First, the geology beneath the three nuclear test locations is very similar; therefore, the groundwater modeling protocols will be similar. Second, the faults between the tests are interpreted to dip steeply. Although the permeability of the faults is unknown, if it is significantly

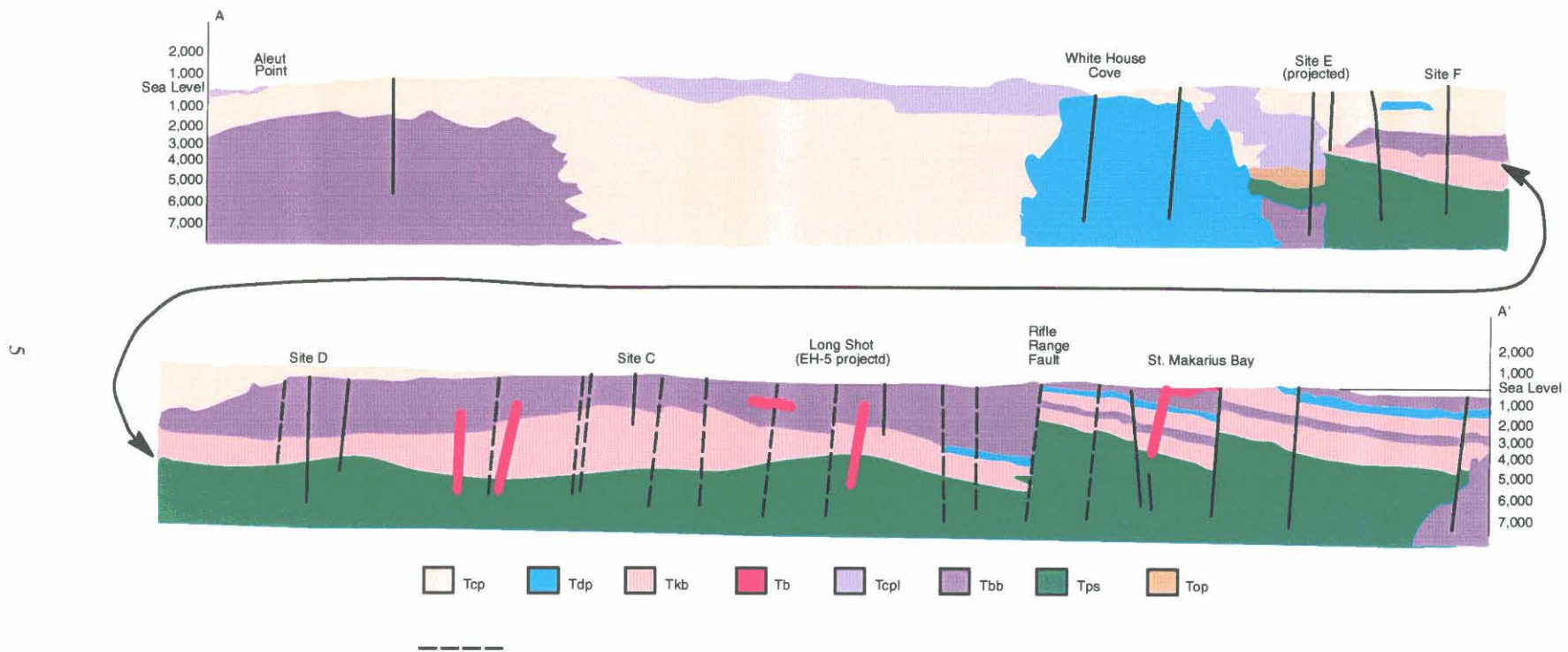


Figure 3. Geologic cross section along the long axis of Amchitka Island (after Carr *et al.*, 1971).

different than the country rock, the effect will be the same: they will effectively separate the regions between faults into discrete hydrogeologic units. If the fault permeability is much lower than the country rock, then a barrier to lateral flow is created. If the permeability is much higher than the country rock, water will flow preferentially toward the faults and depress the water table elevation. This will also cause the transition zone to rise in the faults, and a groundwater divide is created (Figure 4). Thus, each underground test can be modeled as a separate entity that is bounded on either side by faults that transect the island and extend far enough seaward to maintain the groundwater divides. This limits the extent of each of the three models to a width (between faults) of approximately 2 to 4 km (Figure 5).

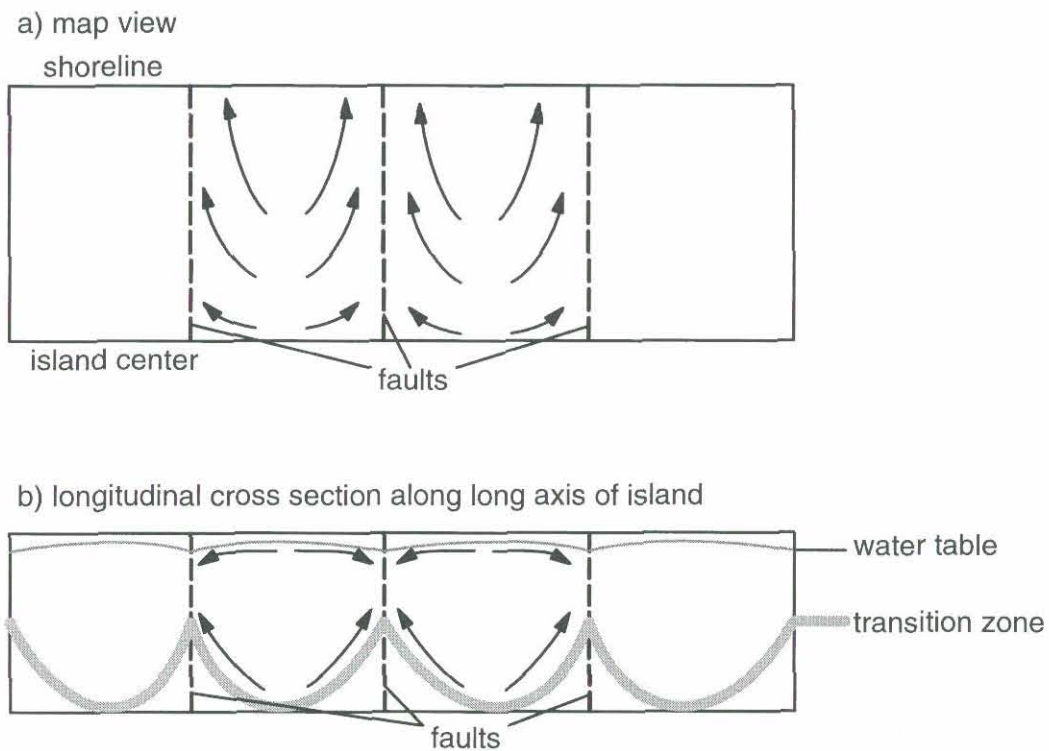


Figure 4. Illustration of groundwater divides created by higher permeability, vertical faults. Not drawn to scale.

Transition Zone

The hydrogeology of Amchitka island is very different from hydrogeology at sites where the density of groundwater is not strongly linked to the concentration of solutes (more accurately, where the range of concentrations is relatively small). An extended “tracer test” has been ongoing beneath the island for as long as there has been an island. The tracer test is embodied in the transition zone, the position and width of which are strongly and directly linked to the mean permeability and effective dispersion coefficient of the rocks that compose the island. At purely freshwater sites, the permeability data typically need to be obtained via direct measurement. The effective dispersion

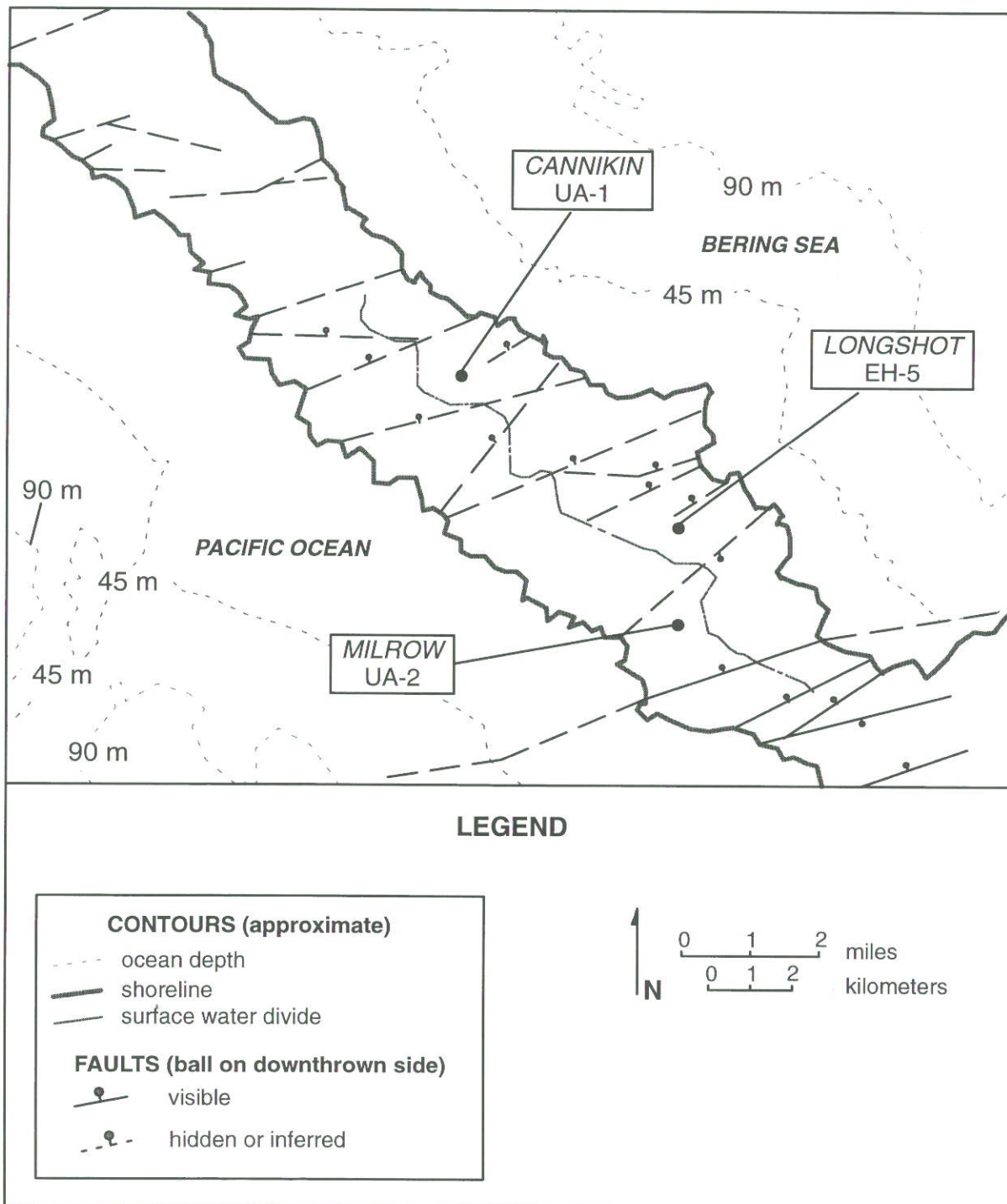


Figure 5. Schematic map of underground testing areas showing major features and bathymetry (after von Huene *et al.*, 1971).

coefficient can be estimated based on the permeability statistics (particularly the spatial correlation) or by a man-made tracer test. An effective dispersion coefficient for the classical advection-dispersion equation grows as a tracer moves and travels through material of variable permeability. Only after the tracer moves many times the distance of the limit of permeability correlation is the dispersion coefficient thought to stabilize. At a typical site, a potential receptor might exist at a range of distances from the radionuclide source, making estimation of a single dispersion coefficient a moot exercise, since any estimation of the parameter is valid for only one scale. Often, the permeability statistical properties are used to generate possible realizations of a given site and the advective transport is solved without any large-scale dispersion. The tracer behavior within many of these realizations is averaged to give estimates of the apparent large-scale dispersion and the uncertainty associated with the prediction. The uncertainty arises also because the tracer has travelled a relatively short distance with respect to the the range of permeability heterogeneity. In this case, the tracer has not had sufficient time or distance to assume an average shape.

At Amchitka Island, relatively few wells were emplaced that can yield sufficient information about the permeability spatial autocorrelation. However, saltwater and freshwater are continuously mixing as they converge at the transition zone and migrate toward the seepage face. If we have information about the degree to which this zone disperses, then we have a direct measure of the degree to which radionuclides will disperse under the same forces, since most of the flow lines beneath the island converge toward, and follow, paths along the transition zone (Figure 6).

The most straightforward method of determining the position and width of the transition zone (hereafter the width refers to the vertical distance between seawater concentrations of 25 and 75 percent near the axis of the island) is to obtain representative groundwater samples from the rock at various depths. At the Milrow site, the transition zone has a depth (the position of 50 percent seawater) of approximately 700 m and a width of approximately 500 m (Figure 7). At the Cannikin site, well water samples obtained from different depths show a different trend, rising to a maximum concentration of about 15 percent seawater at 2,000 m (Figure 8). This would indicate a transition zone depth significantly deeper than 2,000 m. The discrepancy of the measured concentration profiles between the two sites (Milrow and Cannikin) has been attributed to the loss of large amounts of freshwater-based drilling fluid into the Cannikin holes and incomplete purging of the drilling-fluid contaminated water (Fenske, 1972). Other researchers are less convinced that the concentrations measured in the Cannikin wells are due to dilution of the salty formation water by fresh drilling fluid. Dudley *et al.* (1977) contend that the measured profile (Figure 8) in Cannikin wells does indeed show a transition zone located deeper than 2,000 m. The implication of the greater transition zone depth with respect to the ability to model radionuclide transport is great, since the velocity magnitudes are very different above, within, or below the transition zone.

The ability to estimate the position of the transition zone is of primary importance to the proposed modeling effort. Wheatcraft (1995) showed that the position of the transition zone is directly linked to the dimensionless ratio of average recharge (R) to mean hydraulic conductivity (K) of the island's rocks. Hydraulic conductivity can be used instead of permeability because it is not a strong function of salt concentration. Wheatcraft (1995) also showed that an order-of-magnitude change in the ratio $R/K \equiv N_{rk}$ from 2.7×10^{-3} to 2.7×10^{-2} is needed for the

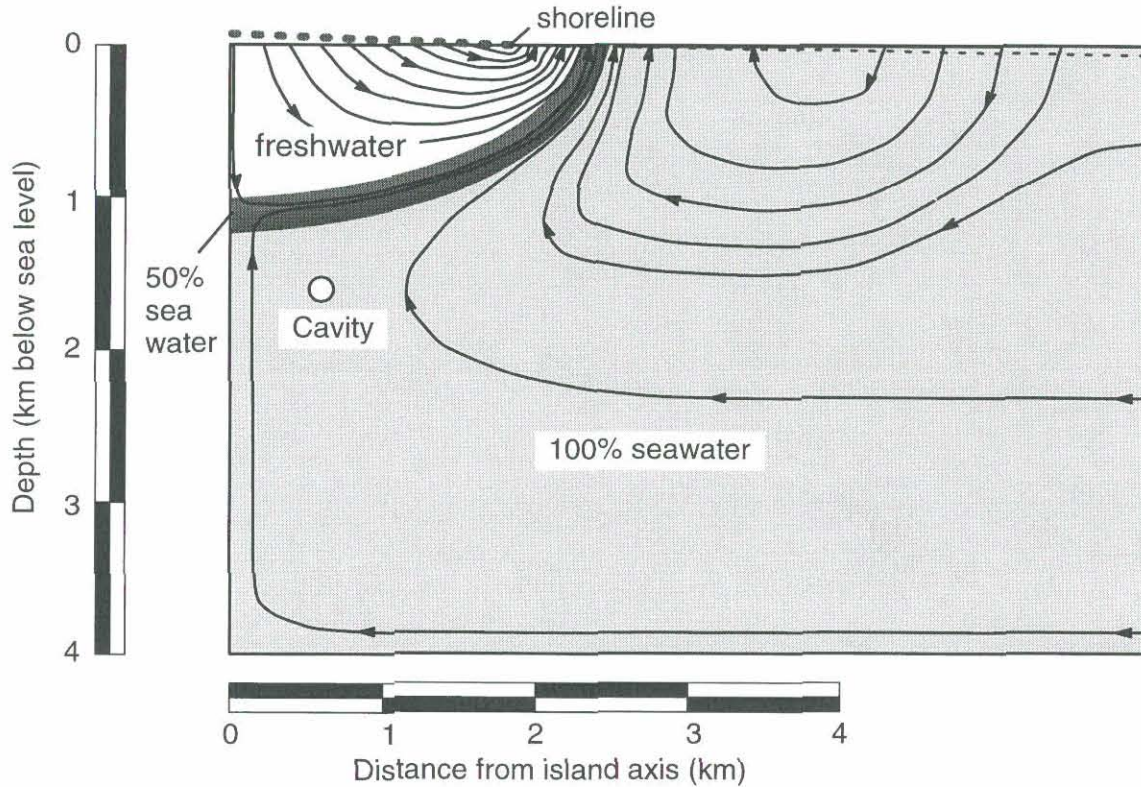


Figure 6. Uniformly distributed streamlines for a dimensionless recharge number $N_{rk} = 10^{-2}$. The approximate island topography and ocean bottom bathymetry are shown by the dashed lines. Approximate location of the Cannikin test cavity is shown. After Wheatcraft (1995).

transition zone to move from a depth of approximately 700 m to 2,400 m. If the chemical analysis of samples obtained from the Cannikin wells is to be believed, then an order-of-magnitude difference between the Cannikin and Milrow areas is required in either the effective recharge, the hydraulic conductivity, or a combination of the two.

In the late 1960s and early 1970s, comparatively little was known about the character of seawater intrusion. The circular “feedback” of the nonlinear governing equations makes analytic solution of the equations for general problems essentially impossible (an exception is the famous “Henry” [1964] problem). At the time of the Amchitka tests, a common assumption was that no salt transfer took place and the interface between freshwater and saltwater was sharp. This implies a static saltwater system.

Fenske (1972) used this assumption and offered static water level data obtained during shut-in tests in different depth zones to support his contention that the transition zone at Cannikin was on the order of 1,200 m below ground surface. His analysis is based on the fact that a piezometer filled with freshwater will show higher-than water table water levels if the well screen is placed in saltwater overlain by a hydrostatic freshwater lens (Figures 9 and 10). Since the formation water below the transition zone is denser than the freshwater in the well casing, more freshwater is needed in the well to equal the pressure at the well screen (Figure 9). The inflection point is at the location

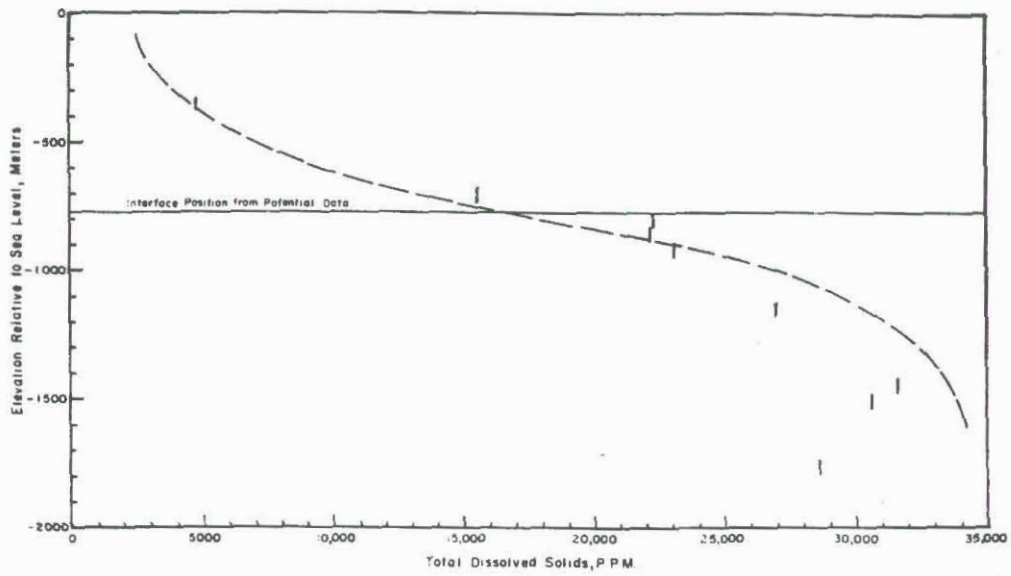


Figure 7. Salinity measured in samples from the Milrow site well UAe-2 (from Fenske, 1972).

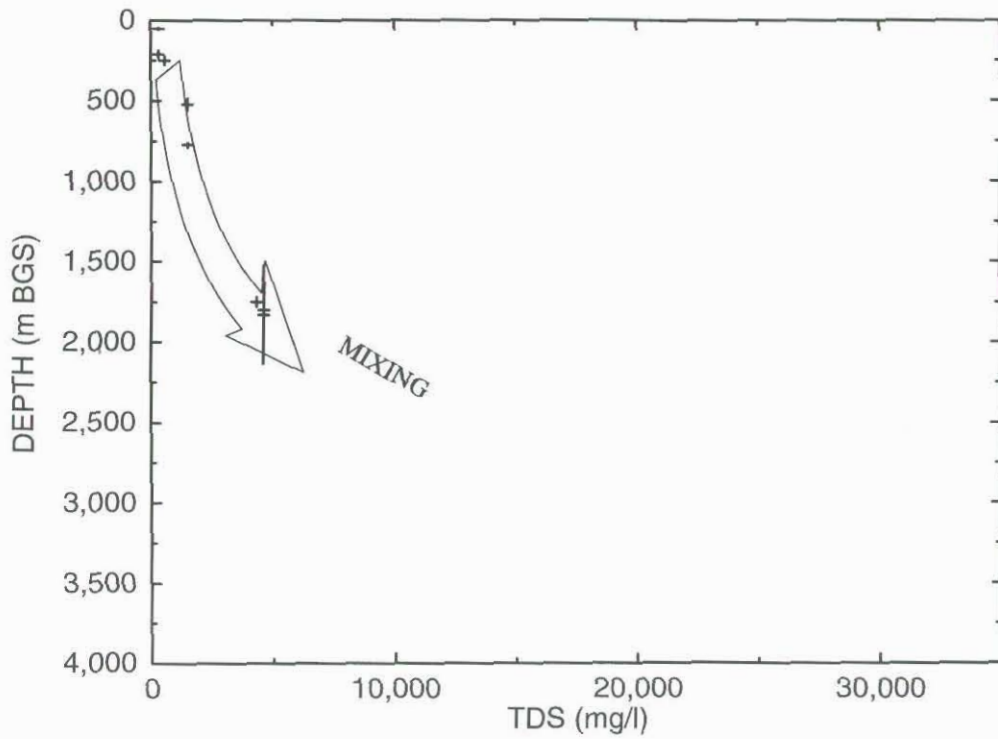


Figure 8. Measured salinity in samples obtained from Cannikin-area wells.

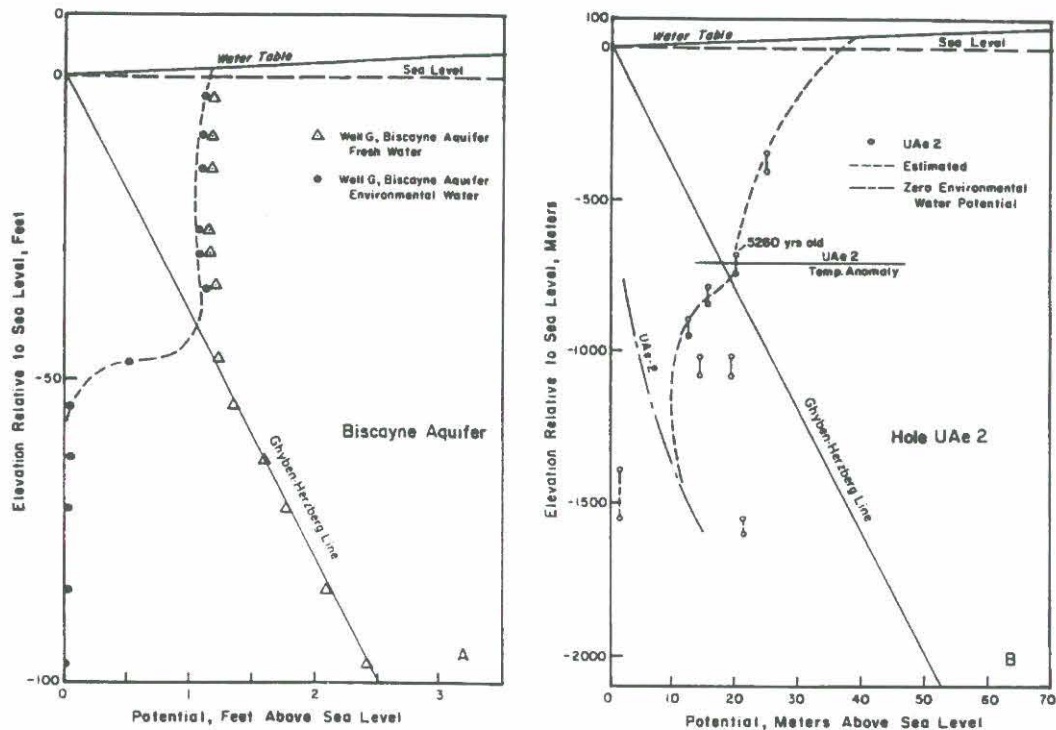


Figure 9. Water levels measured at different depth intervals in (a) the Biscayne Aquifer, Florida, and (b) well Uae-2 (Milrow). Biscayne Aquifer, shown for reference, was measured using fresh water or fully purged “environmental water” in well casing. The inflection point in Uae-2 measurements corresponds to middle of transition zone measured with chemical analyses. From Fenske (1972).

of the sharp interface. On the other hand, if the well was fully purged and filled with the formation water entering the well screen, then the water level in the well would be at the water table if the well screen is above the interface, and approximately 1/40th of the water table elevation if the screen is below the interface. For a non-hydrostatic system, however, the slopes of the lines will not be vertical, and when a transition zone is present, the changes will be gradual (Figure 10b). Further, if the water in the well casing is a mixture of formation water and freshwater (or drilling fluids with density somewhere between the two), the water level observed in the shut-in tests can occupy any portion of the shaded region shown in Figure 10b. The shut-in pressure data for the Cannikin wells presented by Fenske (1972) do not show any inflections and all data lie within the shaded portion of the graph (Figure 10c), so that no conclusions based on concentration or shut-in pressure have yet been confidently reached concerning the transition zone position at Cannikin.

A suite of geophysical logs was conducted in the test wells at Milrow and Cannikin after installation. Most geophysical logs are designed to exploit the difference between the electrical resistivity of the drilling fluid and the formation water. Other logging tools exploit differences in the properties of the rock and the interstitial water. In particular, spontaneous potential (SP) logs register strong negative responses when a fresher drilling fluid invades a layer (or fracture) initially filled with saltwater. No response is registered if drilling fluid enters a fracture that is initially filled

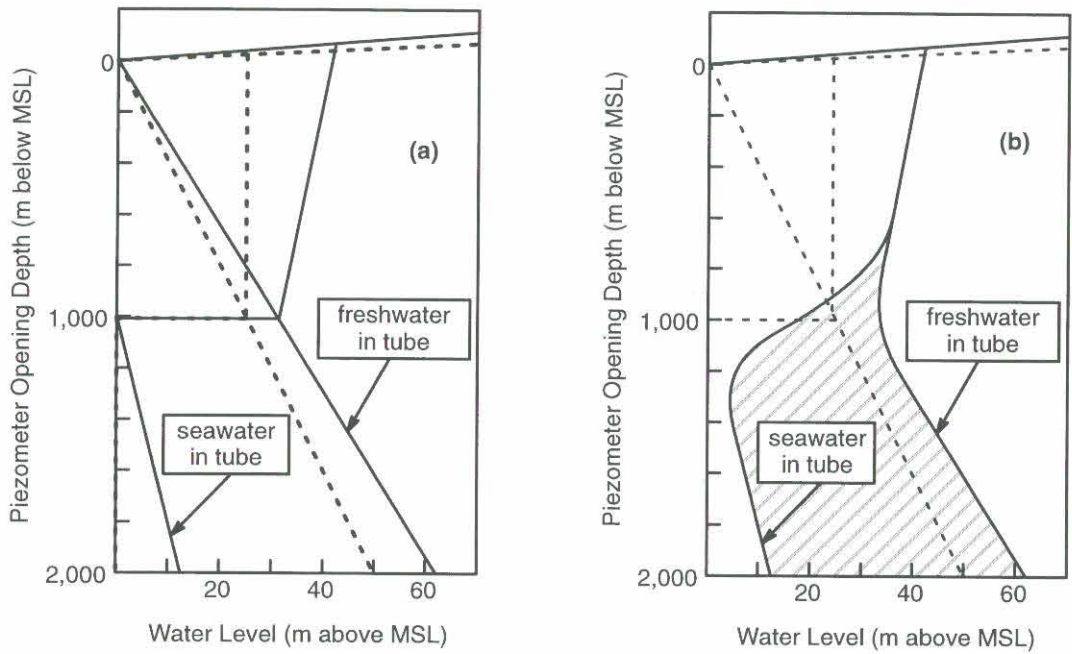


Figure 10. Water levels in piezometers at different depths relative to a saltwater interface: a) sharp interface that is either static (dashed) or circulating (solid), b) dispersed and circulating (dashed lines are the same for reference). The static lens shown by dashed lines is described by the Ghyben-Herzberg relationship. In (a) and (b), the 50 percent seawater elevation (the “interface”) is 1000 m. Mixtures of environmental water and freshwater (*i.e.*, drilling mud contamination) would present elevations in a well within the shaded area. Pressures measured in Cannikin wells are shown in (c), from Fenske (1972).

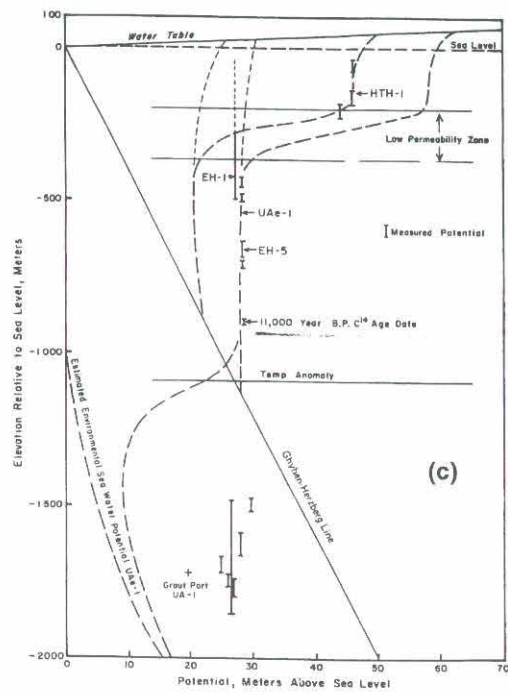


FIGURE 6. Fresh Water Lens, Holes UA-1, HTH-1, EH-1 and EH-5

with water of similar electrical conductivity. Gamma logs, which measure the gamma-ray emission from the formation rock and fluid, may provide a signature of the transition zone. Since seawater is enriched roughly 40 times with respect to potassium (^{40}K is a gamma emitter), high porosity zones that are filled with seawater should have a higher gamma signal, in the absence of potassium-bearing rocks. It is not presently known whether the abundance of potassium in the andesitic rocks have overwhelmed this signal. The fact that many geophysical logs are sensitive to the initial pore water concentration suggests that a careful reanalysis of the electric, electromagnetic, and gamma logs from the Cannikin wells may give valuable information about the transition zone position and width.

Finally, Wheatcraft (1995) showed that the seepage face for both the freshwater lens and the recirculating seawater is relatively insensitive to the lens thickness. The nature of the recirculation suggests that a large percentage of the flowlines converge to a relatively narrow seepage face located within 1 or 2 km of the island shoreline (Figure 6). Nearly all flowpaths beneath the island move more or less vertically (up or down) toward the transition zone and thence to the relatively narrow seepage face. Based on the near-island bathymetry (von Huene *et al.*, 1971), this implies a discharge point for these groundwaters in ocean water less than approximately 50 to 100 m deep (Figure 5).

Permeability

As part of the standard approach to the installation of wells at the Milrow and Cannikin sites, several hydraulic tests were performed to estimate the ability of the formation to conduct water. These tests take the form of swabbing and jetting tests wherein water is quickly added or removed from the well after a section of the casing is isolated via packers. The tests typically do not follow the protocol of constant rate pumping tests or instantaneous slug tests. Rather, rough estimates of overall injection rates and water levels are sometime made and the data are reported in the form of “relative specific capacity” (RSC). RSC has the dimensional form of hydraulic conductivity ($\text{L}\cdot\text{T}^{-1}$), but the link between RSC and hydraulic conductivity is generally considered weak. Reported values of RSC give a rough estimate of the trends that the permeability might be expected to have (Figure 11). For example, RSC values plotted for the Cannikin test holes (UA-1 and UAe-1) show a decrease with depth, a trend that has been attributed to lithostatic compression and closure of transmissive fractures. One should also notice that the RSC values from UA-2 (Milrow site) are similar to UA-1 and UAe-1. The range of RSC values is also fairly narrow in the depths of the nuclear tests. However, we do not anticipate using the reported values of RSC within the proposed modeling effort. A re-analysis of the tests is proposed, since the RSC tests typically used very small amounts of the measured water level data (Figure 12). Some tests were also conducted in such a way that more standard methods of analysis are possible, such as recovery following a constant-rate pumping test or an instantaneous slug test. A re-analysis would allow the assessment of relative accuracy of the given values and would be analyzed in such a way that values of intrinsic permeability would be directly estimated.

One such test, a recovery following a relatively lengthy period of water removal, suggests that the permeability of the rock adjacent to the packer-isolated interval is held in two “compartments” (Figure 13). One of these compartments transmits water relatively quickly, but a significant amount of water is transmitted much more slowly. This is typical of fractured rocks that have significant porosity in the poorly-connected blocks between larger fractures. This observation has broader

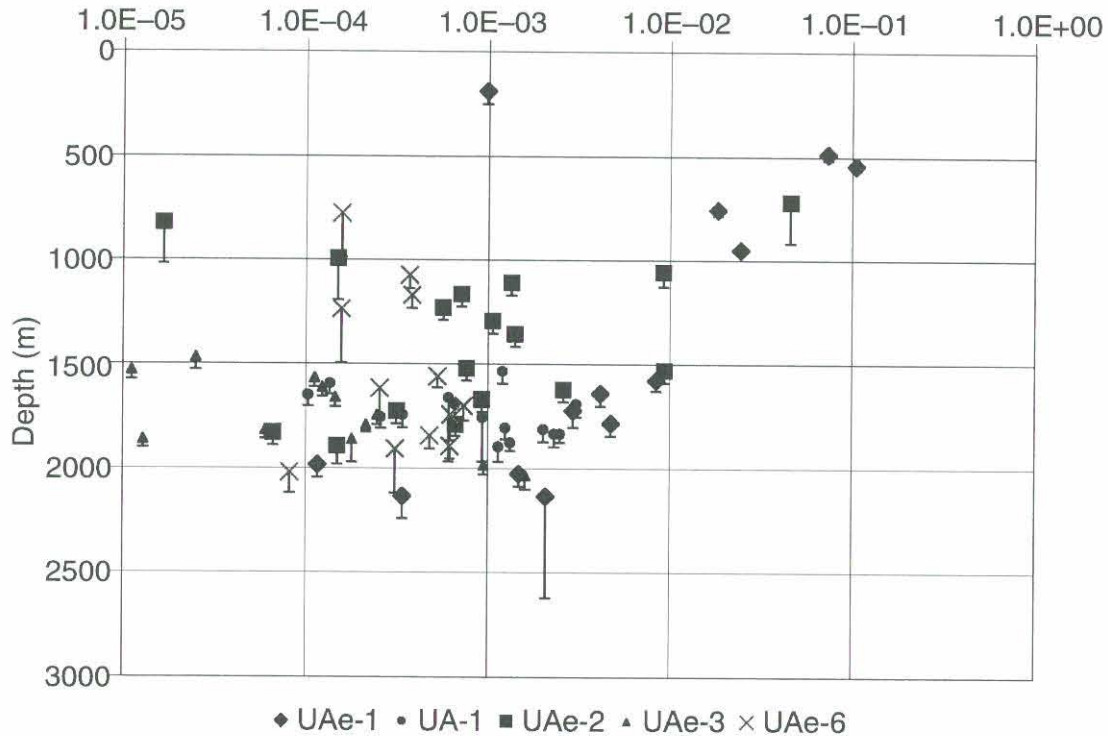


Figure 11. Relative Specific Capacity in packer-isolated intervals. Vertical bars indicate depth zone tested. UAe-6 and UA-e-3 are located approximately 20 and 30 km NW of the Cannikin wells (UA-1 and UAe-1).

implications, since the movement of radionuclides will be similar (qualitatively) to the water in this test: at any moment, a certain portion of the radionuclides will move more rapidly through the well-connected fractures and a certain fraction will move into (or slowly out of) the poorly-connected portion of the whole-rock porosity. The re-analysis of hydraulic tests will be conducted with a mindset of estimating primary versus secondary permeabilities and porosities.

The apparent dual-media are also graphically exhibited in a data set presented by Fenske (1972) in which the water level in UAe-1 was continuously measured simultaneously with the tide in the Bering Sea and the barometric pressure (Figure 14). Very close connection of the water level in UAe-1 to both the oceanic and atmospheric pressure-loading sources indicates that the rapid transmission of pressure is within high conductivity zones with little storage (damping) ability. Fenske (1972) wrote that the data were consistent with a high-permeability fracture porosity on the order of 0.001 and a hydraulic conductivity of 4×10^{-7} m/s ($k \approx 4 \times 10^{-14}$ m²). Connection with the high-porosity, inter-fracture matrix is judged to be poor, since the barometric and tidal signals are only slightly damped.

Recharge

Estimation of recharge on island systems is complicated by the fact that the island has a limited capacity for water. The island builds a lens with a thickness that is limited by the overall permeability. If the permeability is small, the rate at which water can be released at the seepage face

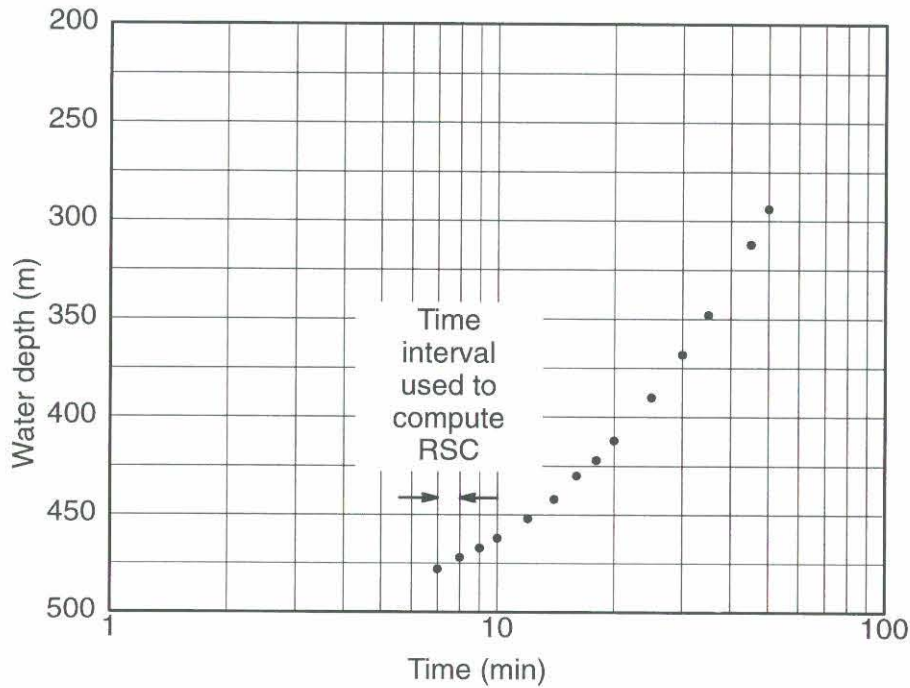


Figure 12. Typical hydraulic test of a packer-isolated zone in well UAe-6h. Note the data interval used to calculate the reported RSC value. Data from Ballance, (1972b).

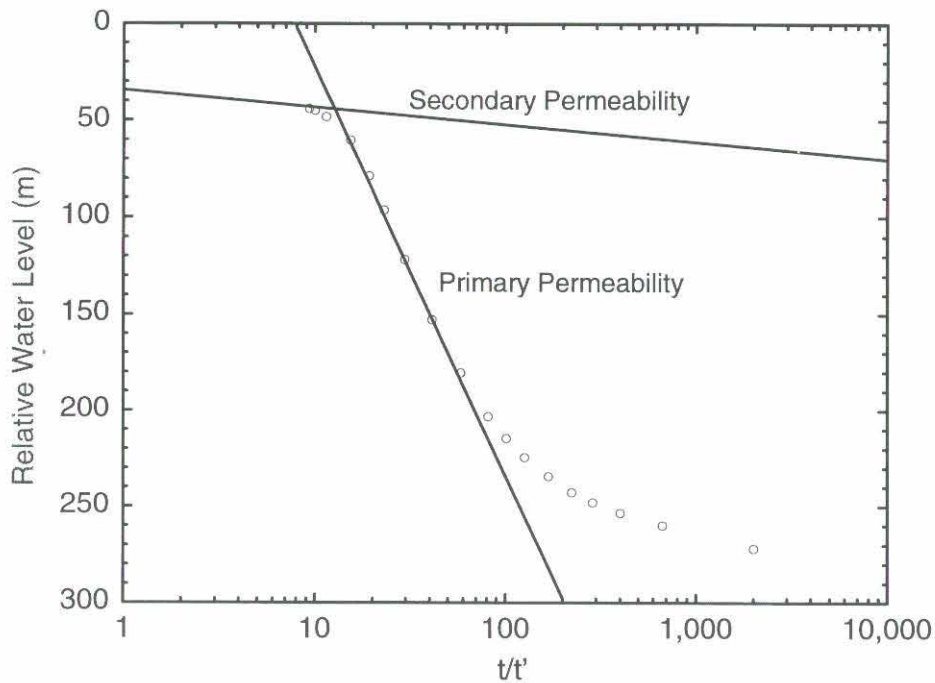


Figure 13. Recovery of water level in well UAe-1 following removal of water from a packer-isolated interval. The recovery is plotted against total time elapsed since pumping started divided by the time since pumping stopped (t/t'). Water level should recover to pre-test level (35 m) as t/t' goes to 1. Data from Ballance, (1972a).

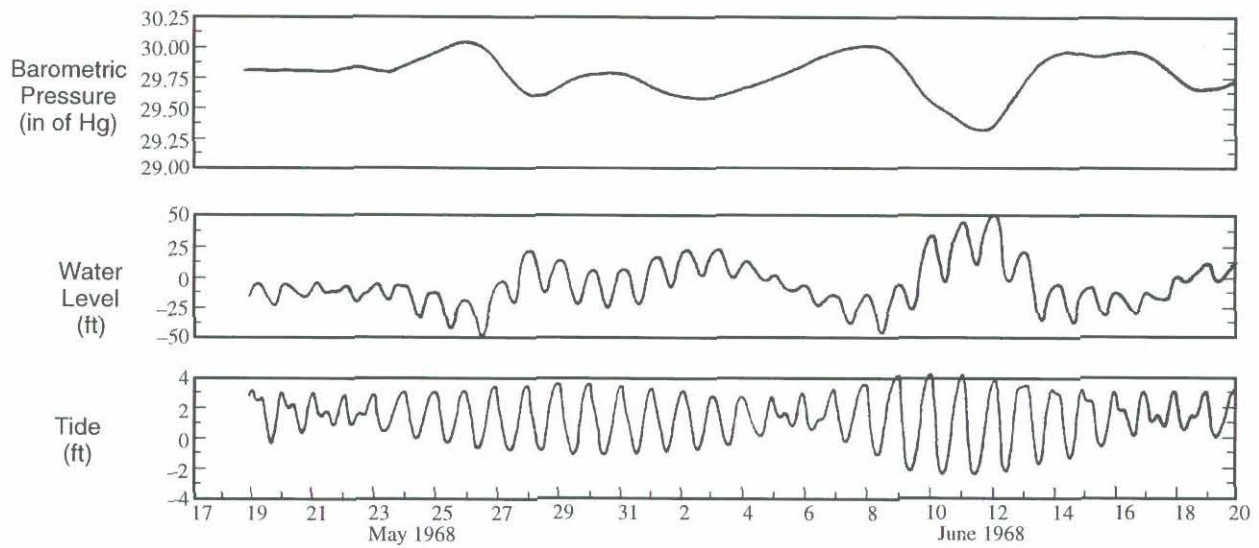


Figure 14. One month response of the water level in well UAe-1 to barometric pressure and tidal fluctuations. After Fenske (1972).

is limited, and a thick freshwater lens develops. If the water table intersects the land surface, a spring or lake results and the amount of recharge is thereby limited to a maximum rate. In effect, the dimensionless variable N_{rk} has an upper bound that depends on the topography of the island. The result is that rule-of-thumb estimates of the precipitation-recharge relationship that have been used in the past (Fenske, 1972; Wheatcraft, 1995) are not accurate. A direct estimate of the amount of recharge can be made using the temperature profiles measured in test wells.

Vertical fluid movement can affect the flux of heat within the earth. Stallman (1960) presented the basic equations for the simultaneous transfer of heat and water with the subsurface and suggested that temperature measurements can provide a means of measuring surface recharge. Bredehoeft and Papadopoulos (1965) present the steady-state solution for heat and fluid flow which is applicable in deeper systems where temporal heat variations become negligible. The differential equation for steady-state, one-dimensional, simultaneous heat and fluid flow through isotropic and homogeneous porous media is given by:

$$\frac{\partial^2 T}{\partial z^2} - \left(\frac{c_0 Q_0 v_z}{k} \right) \frac{\partial T}{\partial z} = 0 \quad (1)$$

where T is the temperature ($^{\circ}\text{C}$), z is the vertical Cartesian coordinate (positive downward, cm), c_0 is the specific heat of the fluid (cal/g), Q_0 is the density of the fluid (g/cm^3), k is the thermal conductivity of the solid-fluid complex (cal/cm-sec- $^{\circ}\text{C}$), and v_z (cm/sec) is the surface recharge (or fluid flux). Bredehoeft and Papadopoulos (1965) provide the solution to the above equation as:

$$\frac{(T_z - T_0)}{(T_L - T_0)} = \frac{\exp\left(\frac{\beta z}{L}\right) - 1}{\exp(\beta) - 1} \quad (2)$$

where T_0 is the temperature at the uppermost elevation ($^{\circ}\text{C}$), T_L is the temperature at the lowermost elevation ($^{\circ}\text{C}$), T_z is the temperature at a vertical location z (cm), L is the total vertical thickness over which the analysis is performed, and $\beta = c_0 \rho_0 v_z L / k$ is a dimensionless parameter that is positive or negative depending on whether v_z is downward or upward. The v_z term is determined by non-linear optimization techniques that search for a value of β (and associated v_z) such that there is a minimum difference between the ensemble observed and simulated temperature profile. Because the vertical component of the freshwater fluid flux is expected to decrease with depth in the density-dependent system, the analysis was limited to the highest portion of the measured profiles.

This model has been fit to the temperature profiles in wells at the Milrow and Cannikin sites and roughly 10 and 20 km “up-island” to the northwest (Table 1). The model shows reasonably good fit to the upper portion of the curves (e.g., Figure 15). The recharge values interpreted from the four temperature profiles are many times lower than those used by other researchers. For example, Wheatcraft (1995) assumed a value of 10 cm/yr. The present analysis suggests that the permeability values interpreted for the island from his analysis should be decreased by a factor of six or more.

Table 1. Estimated recharge rates based on the shallow temperature profile.

Well	Estimated Recharge (cm/year)
UAe-1	1.6
UAe-2	0.4
UAe-3	1.5
UAe-6h	5.0

Heat-dependent Groundwater Density

The density of groundwater is not an exclusive function of the salt concentration. Warm water is less dense than cold water, although at temperatures commonly encountered in groundwater modeling studies, this is a secondary effect. More precisely, reasonably high temperature gradients are required before heat-dependent transport is possible. This transport takes the form of unstable convection, when warm water initially underlies cold water in an unstable configuration. If the temperature contrasts are high enough, gravity acts upon the buoyancy difference and drives the warmer water into the cold, giving rise to convective cells. These cells are sometimes manifest on the earth’s surface as hot springs. Lopez and Smith (1995, 1996) have studied the flow of groundwater and heat in terrestrial mountain-block fault systems and found that a narrow set of parameters (heat flow, natural groundwater velocities, and permeability) are conducive to natural heat convection. The natural conditions beneath Amchitka Island are not likely to fall within the

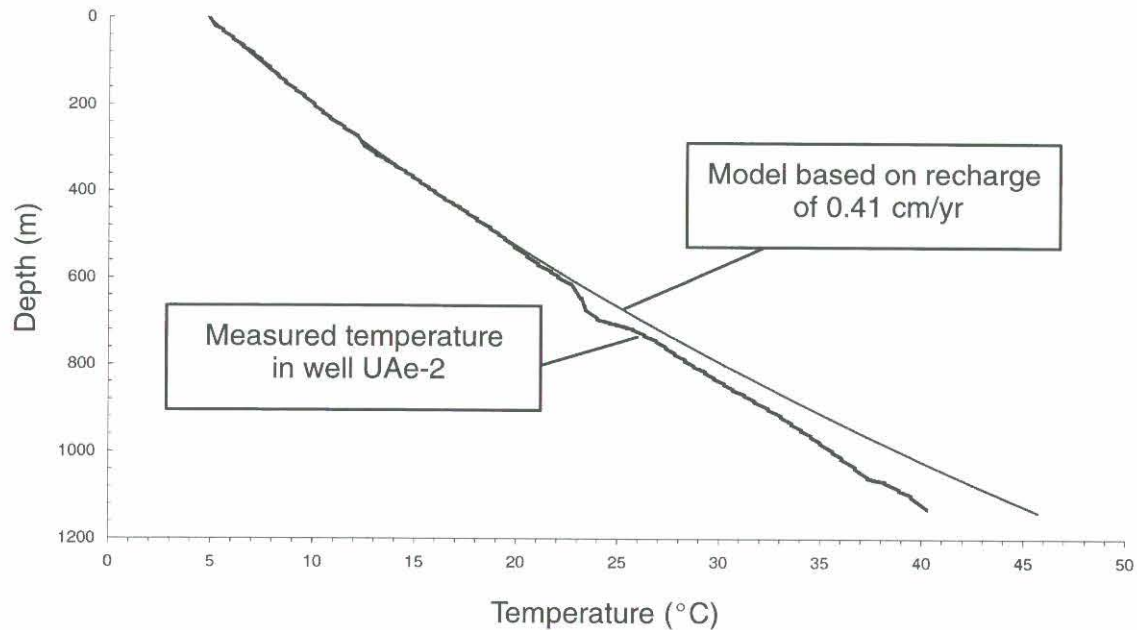


Figure 15. Estimation of recharge based on temperature deflection measured in well UAe-2 at the Milrow site.

narrow parameter space, since no surface evidence of convection (hot springs or hydrothermal alteration along the fault zones) has been reported.

A recent study by an international advisory committee (IACWG4, 1998) showed that natural convection was possible at the Pacific atoll of Mururoa. The convection was due to the steep flanks of the atoll providing a mechanism for placing cold, deep (1,000s of meters) seawater in close lateral proximity to groundwater that was warmed by geothermal heat flow. Amchitka Island's more gently dipping flanks and lower permeability rock types (compared to the carbonate atolls) decrease the potential for geothermal heat-induced convection. However, the possibility will not be dismissed in the proposed modeling effort.

The emplacement of hot water in the test cavities may provide the impetus for local convection or enhanced vertical flow up towards the transition zone (for tests conducted below the transition zone). The aforementioned study of groundwater flow beneath the Pacific atolls suggests that the potential for local buoyant flow is reasonably high for several hundred years. This potential can be assessed in a preliminary fashion by estimating the Rayleigh number for buoyant instability given by the measured temperature profile in the Cannikin well UA-1-P1 (Figure 16). The Rayleigh number is a measure of the driving forces (permeability, temperature contrast, gravity, etc.) divided by damping forces (thermal diffusivity, viscosity). Rayleigh numbers greater than approximately 40 indicate an unstable configuration. Using reasonable estimates of the physical properties of water, a permeability value for the chimney of ten times that given by Wheatcraft (1995) for the natural rock, and the temperature profile measured several hundred days after condensation of steam within the test cavity, a Rayleigh number of roughly 60 results. This should be considered a maximum value, since Wheatcraft's (1995) estimate of the permeability is based on a recharge rate of 10 cm/yr.

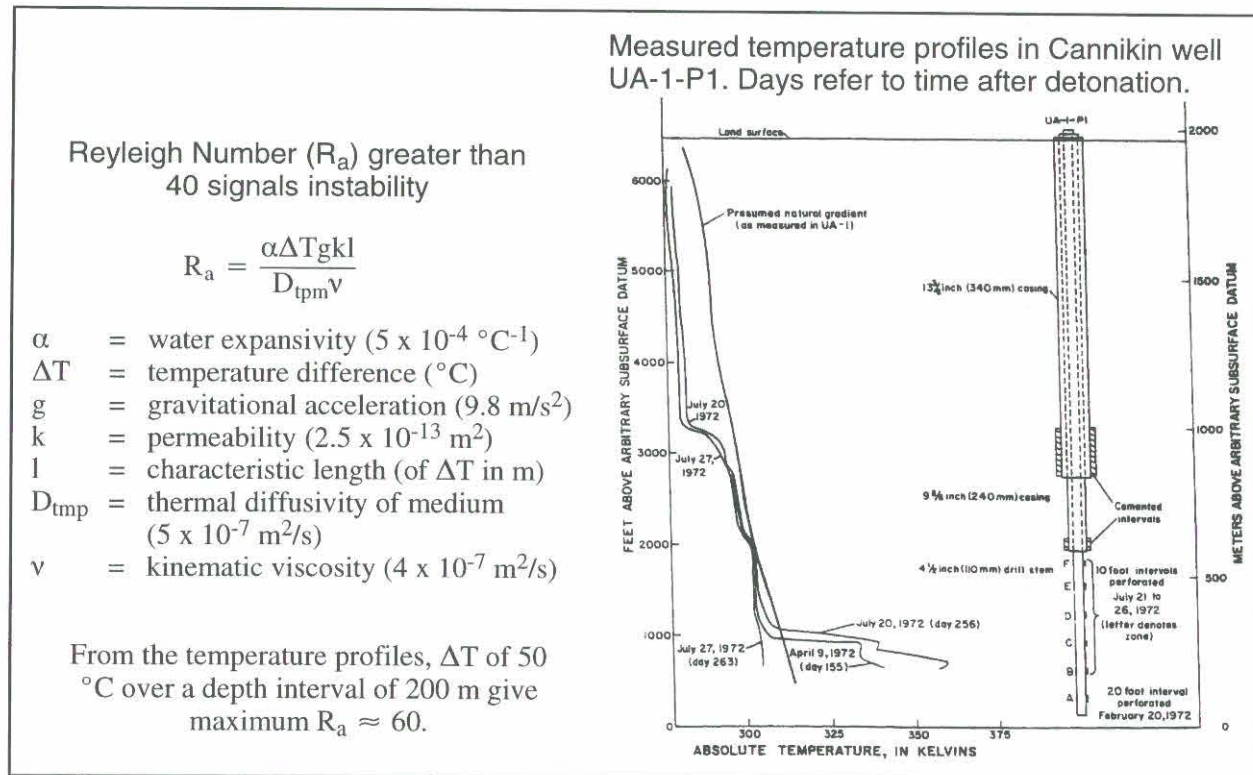


Figure 16. Rayleigh number estimates for the UA-1-P1 temperature profile (figure after Claassen, 1978).

Lower values of recharge would yield commensurately lower values of permeability from Wheatcraft's analysis. This analysis suggests that the potential for heat-dependent convection within the chimney is small; however, estimates of the permeability may change throughout the modeling effort. Some simplified simulations of heat and salt transport will be performed to assess the impact of heat-driven or *heat-aided* alteration of the flow field.

PROPOSED MODELING EFFORT

Numerical Considerations

Numerical approximation of the coupled flow and transport problem is inherently time-consuming. The flow (pressure) field must be continually re-solved as tracer and saltwater moves, since changes in salt concentration result in changes in water density (Figure 17). This is in contrast to density invariant solute transport, in which the flow field is solved only once. The continual recalculation of the flow field in the saltwater intrusion problem imposes a serious limitation on the number and size of simulations that feasibly can be accommodated. Furthermore, because the velocity field can vary sharply in space, Lagrangian (particle tracking) algorithms introduce a form of artificial dispersion that can change the flow field (Benson *et al.*, 1998), so finely discretized Eulerian transport codes are more favorable. The underlying flow (velocity) field must be solved on a grid on the order of the local dispersivity, whereas density-invariant problems that use particle tracking can solve for pressure and velocity on a much coarser level. One can assume

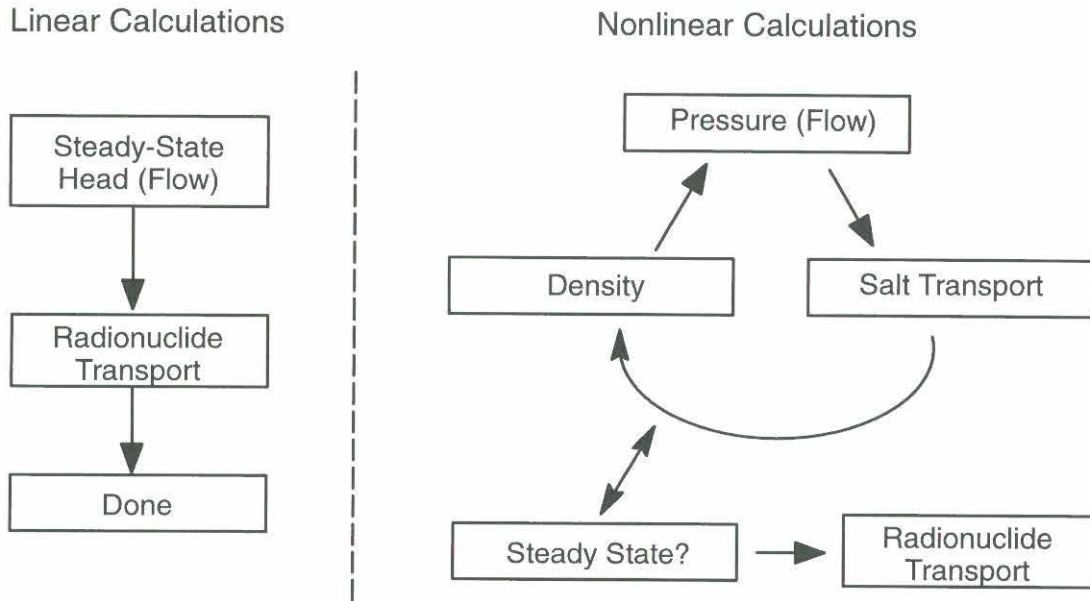


Figure 17. Illustration of the inherent differences in the computational load of linear versus nonlinear flow and transport models. If relatively steady-state conditions are not reached prior to radionuclide transport, the computational difficulty for the nonlinear problem grows very high, since the arrow goes both ways continually.

that a density-coupled flow simulation will consume much more computer time than an equivalently discretized density-invariant solute transport model, and the multiplier grows larger as the number of elements grows.

Typically, iterative solvers become slower at a rate of $n \times \ln(n)$, where n is the number of elements (or finite difference blocks). Modern direct solvers become slower at a rate of roughly n^2 . Added to this is the constraint that smaller grid elements require more timesteps, since the timestep size is limited by the Courant number. This increases the calculation time by another factor of (n) . So each tenfold increase in the number of elements will cause the program to run hundreds to thousands of times slower, depending on the solver. Therefore, three-dimensional (3-D) solutions are necessarily hundreds or thousands of times slower than 2-D. Conversely, hundreds or thousands fewer analyses can be performed in 3-D.

The number of elements clearly must be minimized to keep the analyses tractable. Theoretically, a finite-element simulation is favored, since the elements can be shaped arbitrarily. The mesh can be made fine in the areas of active transport (high concentration gradients) in the transition zone, and coarse in relatively quiescent areas, such as the far seaward boundary of the domain. Finite-difference schemes suffer from the fact that the grids must be continuous and orthogonal, so small grid sizes extend across the entire domain.

The proposed scope of work is based on a plan to assess the impact of various physical parameters on the transport of radionuclides beneath Amchitka Island toward the ocean. These parameters or modeling constraints include 1) model dimension, 2) recharge rate and variability, 3)

bathymetry (*i.e.*, definition of boundary conditions), 4) permeability distribution, 5) hydrodynamic dispersion, 6) porosity (and multi-mode porosity), 7) thermal buoyancy, and 8) radionuclide reactivity (transformation and rock interaction). Perfect knowledge of all of these parameters is impossible, which leads to parameter uncertainty. Clearly, the parameter space cannot be completely investigated because of the number of parameter dimensions. For example, using four different “values” of each of the eight parameters or constraints results in 4^8 (65,536) simulations. This limitation suggests that the impact of uncertainty of several parameters must be assessed independently of others. Of course some of the parameters have little or no uncertainty for some values of a constraint (*i.e.*, bathymetry is well known in 3-D, but variable or uncertain in 2-D).

Code Availability and Capability

A large number of codes are available that can simulate one or more of the processes that have been identified as potentially important to radionuclide transport beneath Amchitka Island. Many of the codes are optimally designed for specific portions of the problem, or have enhanced capabilities that are attractive for some portions of the proposed work. We have devised a modeling scheme that will capitalize on the optimal performance of some codes to investigate individual aspects of the flow and transport processes. Information gained from the subtasks of the modeling effort will be combined into a final conceptual and numerical simulation of the radionuclide transport. For example, the popular U.S. Geological Survey (USGS) code SUTRA is only available in 2-D and does not simultaneously solve for heat and solute transport. However, third-party grid generation software (such as Argus ONE) allows the creation of 2-D grids that are optimized for the Amchitka solution (Figure 18). This figure highlights two points concerning code capability. First, finite-element solutions are vastly more optimized for the seawater intrusion problem because the

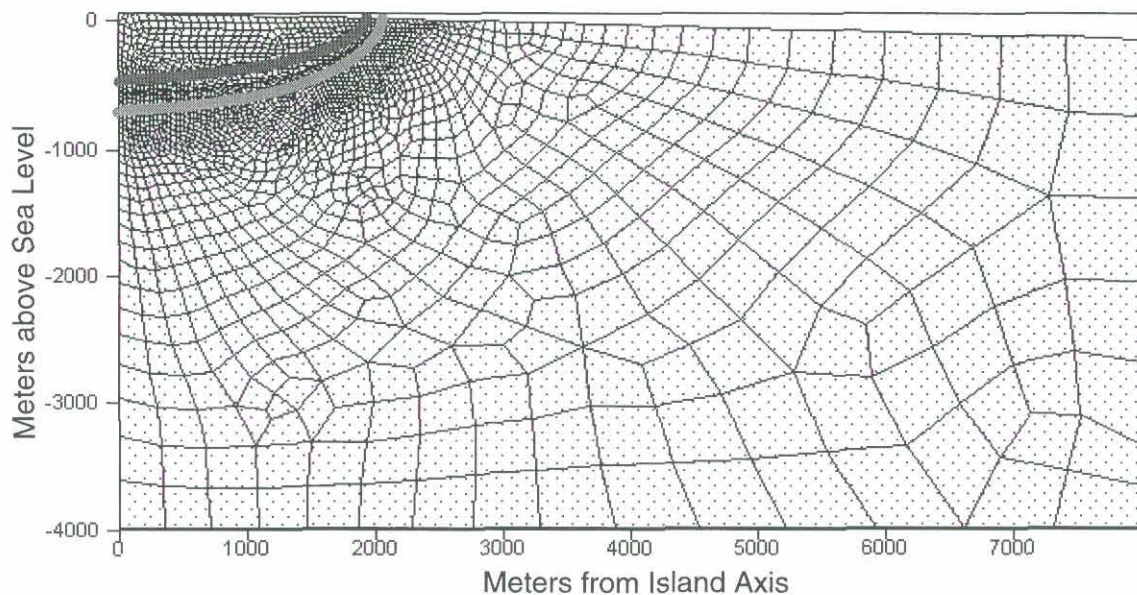


Figure 18. Example grid generated by Argus ONE for a cross section of Amchitka Island. The grid contains approximately 2,000 elements. Elements are roughly 30 m across in the vicinity of the transition zone. Thick curves are iterated steady-state concentration of 25 and 75 percent seawater.

elements can be made very small throughout the transition zone region without unduly raising the number of elements (and the computational difficulty). Second, the geometry and parameters can be varied almost instantaneously in the graphical user interface (GUI) environment and the results easily compared. For these reasons, the finite-element code SUTRA, with the Argus GUI, is considered the optimal platform for most of the proposed simulations.

Matrix Diffusion

Another capability that will be required is a code that can transport dissolved species in the presence of significant matrix (immobile) porosity. Fenske (1972) indicates that while bulk permeability is controlled by fractures, the fracture porosity is relatively small. The bulk of the porosity is derived from intergranular void space. In a continuum solute transport model, this discrepancy between water storage and transmission is typically handled by multi-compartment (essentially bi-modal) velocities. Transport in between transmissive fractures is much slower than within the fractures, and is approximated by a diffusion-limited process. This process is usually called “matrix-diffusion.” Several codes are capable of simulating this process in addition to density-coupled flow. The popular density-coupled transport code (TOUGH2) from Lawrence Berkeley National Laboratory will not be used because it cannot simulate hydrodynamic dispersion in 3-D, irregular meshes. Two other readily available codes (FEFLOW and FEHM) are capable of simulating both density-dependent flow and transport (including hydrodynamic dispersion) with matrix diffusion. Since there are no essential differences in the capability of these two codes, we will only consider FEHM (from Los Alamos National Laboratory) for future use. Many off-the-shelf codes solve chemical transport with matrix diffusion, but do not solve the density-coupled (saltwater) nonlinear equations. These codes can be given the velocity field from one of the density-coupled flow and transport simulations to solve the radionuclide transport in a steady-state flow field. A summary of the selected codes and their pros and cons is given in Table 2.

Geometric Study

The first model “parameter” is spatial dimension. This reduces to a determination of the appropriateness of a 2-D simplification. Previous studies of seawater intrusion have concentrated on the vertical dimension parallel to prevailing flow, or a vertical slice of material perpendicular to a shoreline. These two dimensions are required because gravity of the component generates the dipping interface between the freshwater and seawater, and flow within the lens and the intruding seawater occurs primarily toward the ocean. The 2-D assumption requires that the solution is essentially the same along the long axis of the island in the near vicinity of a particular test. This further assumes that 1) the boundary conditions are consistent and perpendicular to flow; and 2) the faults (and the rubble chimneys) do not significantly change the flow configuration in the manner shown in Figure 4. The first subtask of the modeling effort is to assess the significance of each of these scenarios. This will be done using a simplified 3-D density-coupled flow and transport model and placing parallel faults extending from the island center seaward (Figure 19). We anticipate that the USGS 3-D finite-difference heat and solute transport code HST3D will provide the most straightforward modeling of this scenario, although the limitations presented by the finite-difference method may require the more sophisticated capability of the FEHM code.

Table 2. Comparison of capabilities of selected codes.

PROs	CONs
SUTRA (<u>sat/unsat transport</u>): U.S. Geological Survey	
Finite Element	2-D (presently)
Graphical User Interface (present and future use)	Solute OR Heat
Fast Solver (WATSOLVE)	No Dual Media (matrix-diffusion)
HST3D (<u>heat and solute transport in 3-D</u>): U.S. Geological Survey	
Graphical User Interface	Finite Difference
Heat AND Solute	No Dual Media (matrix-diffusion)
3-D	
FEHM (<u>finite-element heat and mass transfer</u>): Los Alamos National Laboratory	
Finite Element	Interface and mesh generation on SUN platform - may be proprietary?
Heat AND Multiple Solutes (density coupled, uncoupled)	
3-D (maybe a CON)	
Dual Media by Direct Solution (elegant, simple)	
Various Uncoupled Dual Media Transport Codes	
Take velocity field or streamtube(s) from previous density-coupled models	Not a single solution to flow and transport: Requires steady-state flow field
Solve only radionuclide transport	
Variability and uncertainty of matrix properties	

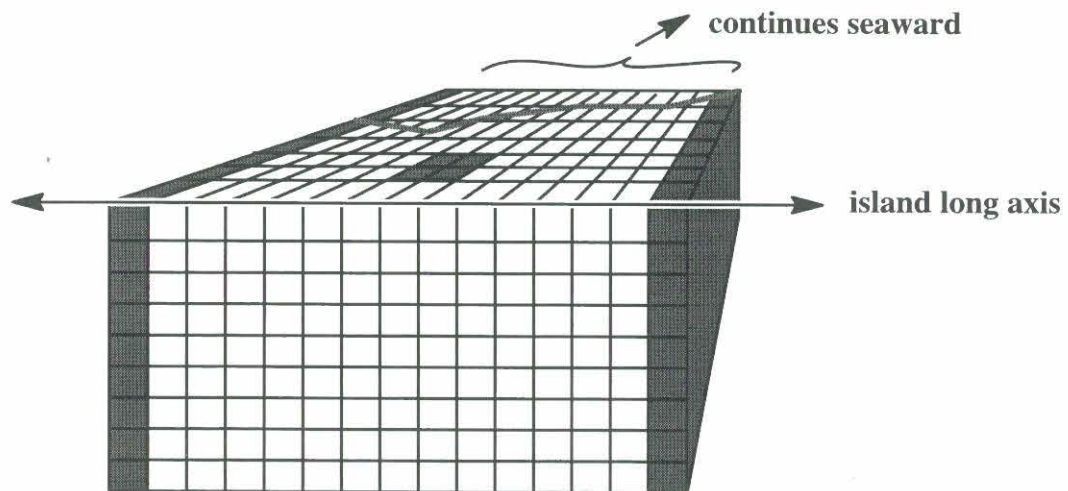


Figure 19. Schematic representation of geometric study. Shaded areas denote higher permeability than country rock. Irregular line denotes non-uniform shoreline (transition from recharge to hydrostatic seawater boundary condition). Not drawn to scale.

The permeability of the idealized faults and chimney are unmeasured quantities. They will be given permeability of 10 to 100 times the country rock permeability, to the extent that the known transition zone position near the test holes can be reproduced. The velocity profile along the typical streamtubes from the cavity position to the seepage face will be compared to the base case (2-D and no faults) for ranking the ultimate effect of the faults. The ranking will be used to determine whether faults and spatially variable boundary conditions (BCs) are to be included in the final simulations.

The ocean bottom depth also deviates from a planar (3-D) or linear (2-D) feature. The true ocean bathymetry will be incorporated into a 2-D model and compared to a linear simplification. Also, results from 3-D and 2-D models identical in all respects except for the bathymetries will be similarly compared. If the velocity along a streamtube from the cavity deviates significantly (by rank with the other parameters), then the true bathymetry will be incorporated into the final model. We do not expect that placing the true bathymetry will be difficult in 3-D.

Geothermal Heat

Following an evaluation of the ease with which the 3-D codes (HST3D and FEHM) can be implemented, the suitable model will be used to rank the effects of geothermal versus ocean water temperature and also the effect of hot cavity water on the long-term velocity field.

Mean Recharge, Permeability, and Dispersivity

Comparatively little is known about the spatial distribution of permeability. Figure 11 shows that the relative specific capacity distribution is similar from the Cannikin wells to the Milrow wells. This trend may change significantly with a re-analysis of the hydraulic testing data. In any case, the sparsity of permeability data precludes a meaningful analysis of the permeability statistical properties. Fortunately, the position of the transition zone is a strong function of the permeability. This allows the permeability and large-scale dispersivity to be used as calibration parameters. Large-scale trends deduced from the interpretation of the hydraulic tests reconciled with the geologic setting associated with rock deposition will be used in 2-D models in an iterative fashion. Measured permeability will be adjusted sequentially to match the observed transition zone position. As discussed by Wheatcraft (1995), the mean permeability and mean recharge are linked to freshwater lens thickness. These two parameters can be combined into a single dimensionless parameter. For lack of contrary evidence, the recharge will be considered spatially constant within a simulation. As previously discussed, the permeability spatial variability gives rise to spreading of concentration (salt or radionuclides). Since the transport is large scale and always to the same point, an effective dispersivity that describes the system is appropriate. The dispersivity will be adjusted to match the width of the transition zone at each test.

Matrix Diffusion

The mathematical description of matrix diffusion ultimately relies on two parameters: matrix diffusivity and porous block length. These parameters control how fast and how far the solute will travel away from the primary fractures that are responsible for advective transport. It is anticipated that these two parameters will be random and known with a degree of uncertainty. Samples of the core taken during emplacement of the Milrow and Cannikin wells are available for laboratory testing

of the diffusivity of solutes within the interfracture porous blocks. It is expected that the diffusivity will be a primary function of the tortuosity within the blocks, and that solute properties will be of secondary importance. The porosity of the blocks is also of secondary importance due to the apparent uniformity of reported porosity (e.g., Lee, 1968). The overall (primary) porosity is another parameter that will be re-analyzed after appropriation of the geophysical logs. The effective length of the blocks can only be discerned by inspection of the core, geophysical logs, and rock outcrops.

These two parameters are important to the breakthrough of contaminant at the seepage face because of the large overall portion of the groundwater that fills the porous blocks and remains essentially immobile. The blocks have a large capacity for accepting and storing radionuclides while they decay. But since these parameters have a random component that is coupled to a velocity field that changes along a streamtube, a numerical solution is required. It is important to note that the matrix diffusion does not enter into the salt transport calculation if the transition zone is in a relatively steady state, since the salt (at whatever concentration) will have diffused fully into the porous blocks. If temporal effects are judged to be unimportant in prior simulations, then the streamtubes can be extracted from the flow simulations and solved independently with an off-the-shelf transport code with matrix diffusion capability (Figure 20). This procedure will vastly reduce the computational load, since the nonlinear flow and salt transport needn't be solved during the anticipated 1,000-year period of radionuclide transport simulation.

Temporal Effects (Recharge and Nuclear Test-induced Heat)

These parameters are discussed last because of the ramifications of their potential effect. The previous section explained that if steady-state conditions were an appropriate assumption, the complexities of radionuclide transport with matrix diffusion could be decoupled from the flow and salt-transport simulation. On the other hand, if the radionuclides are being transported within a velocity field that is highly variable in time, then the radionuclide transport (with matrix-diffusion) must be embedded within continual recalculation of the flow field that is coupled to the groundwater density. This represents an added level of numerical effort that is outside of the scope of the FY99 task plan. If the 3-D effects are also significant, then the indicated modeling effort includes 3-D finite-element, density-coupled flow and transport of multiple chemical species with matrix diffusion. This is clearly a monumental task, with computational effort on a par with modeling efforts at Yucca Mountain. If temporally variable modeling is indicated, the Desert Research Institute will make recommendations for the completion of such work and submit an appropriate proposal for the additional work.

Two parameters have the potential of causing significant temporal variability in the flow field: 1) test-derived, heat-dependent buoyant flow, and 2) temporally variable recharge.

The study of transport at the Pacific atolls (IACWG4, 1998) suggested that buoyant movement of the test-heated water was significant over a period of hundreds of years. The vertical velocities in the chimney were shown to increase by a maximum factor of 3 to 4 for tens of years and decay slowly to pre-test levels on the order of hundreds of years. The hydraulic conductivity (and volcanic rock type at the cavity depth) in the IACWG4 atoll study was similar to that estimated by Wheatcraft (1995) at Amchitka Island. Wheatcraft's permeability values may be too high based on the recharge rates, so advective or convective heat flow at Amchitka Island is probably much less likely than at

the atolls. Nevertheless, simplified simulation of heat flow in the chimney will be conducted using HST3D. The difference in the total travel time from the cavity to the seepage face with and without heat flow will be assessed and ranked with the other parameters. If heat flow is a primary factor in the overall transport of radionuclides, then the modeling effort requires rescoping.

The mean recharge is linked to the mean permeability in establishing the thickness of the freshwater lens. Recharge that varies in time will tend to produce rapid pressure changes that will propagate to the transition zone. This is a potential effect because of the ability of the low porosity fracture system to transmit a pressure pulse over large distances. The USGS code SUTRA will be modified to allow time-variable boundary conditions. A random recharge function will be generated and the relative effect on the velocity field within a streamtube will be evaluated. Significant effects relative to other parameters will signal a rescoping of the modeling effort due to the same constraints as time-variable, heat-induced transport.

Overall Modeling Procedure

Before investing an excessive amount of time in the modeling procedure, all hydraulic tests deemed reasonably properly conducted will be re-analyzed. Geophysical logs that have been procured will be analyzed with respect to transition zone position and width. In the absence of temporally variable flow conditions, the following procedure will be used to model the movement of radionuclides from the three test cavities to their respective seepage faces. At each location:

- Use SUTRA to create 2-D “base case” with chimney permeability and calibrate with geologically controlled permeability distribution;
- Modify SUTRA to allow time-variable recharge and model reasonable yearly-to-decadal recharge variability. Assess convergence to steady state and compare travel time to that of base case;
- Create 3-D “base case” with chimney permeability using HST3D;
- Add idealized faults to 3-D base case and compare overall advective travel time from cavity to seepage face (travel time);
- Add spatially variable shoreline boundary condition to 3-D base case and compare travel time to that of base case;
- Model nuclear test heat- and salt-dependent density flow fields with HST3D and compare travel time to that of base case;
- Model geothermally derived heat- and salt-dependent density flow fields with HST3D and compare travel time to that of base case;
- Reject the parameters which have minor effect in relation to others and construct overall simulation incorporating the parameters whose inclusion showed major effect on travel time. If temporally variable flow and transport is a major factor in the overall flow and-transport, the project must be retasked.
- Generate flow field based on major parameters that is consistent with known transition zone (Figure 20). This may be 2-D or 3-D;

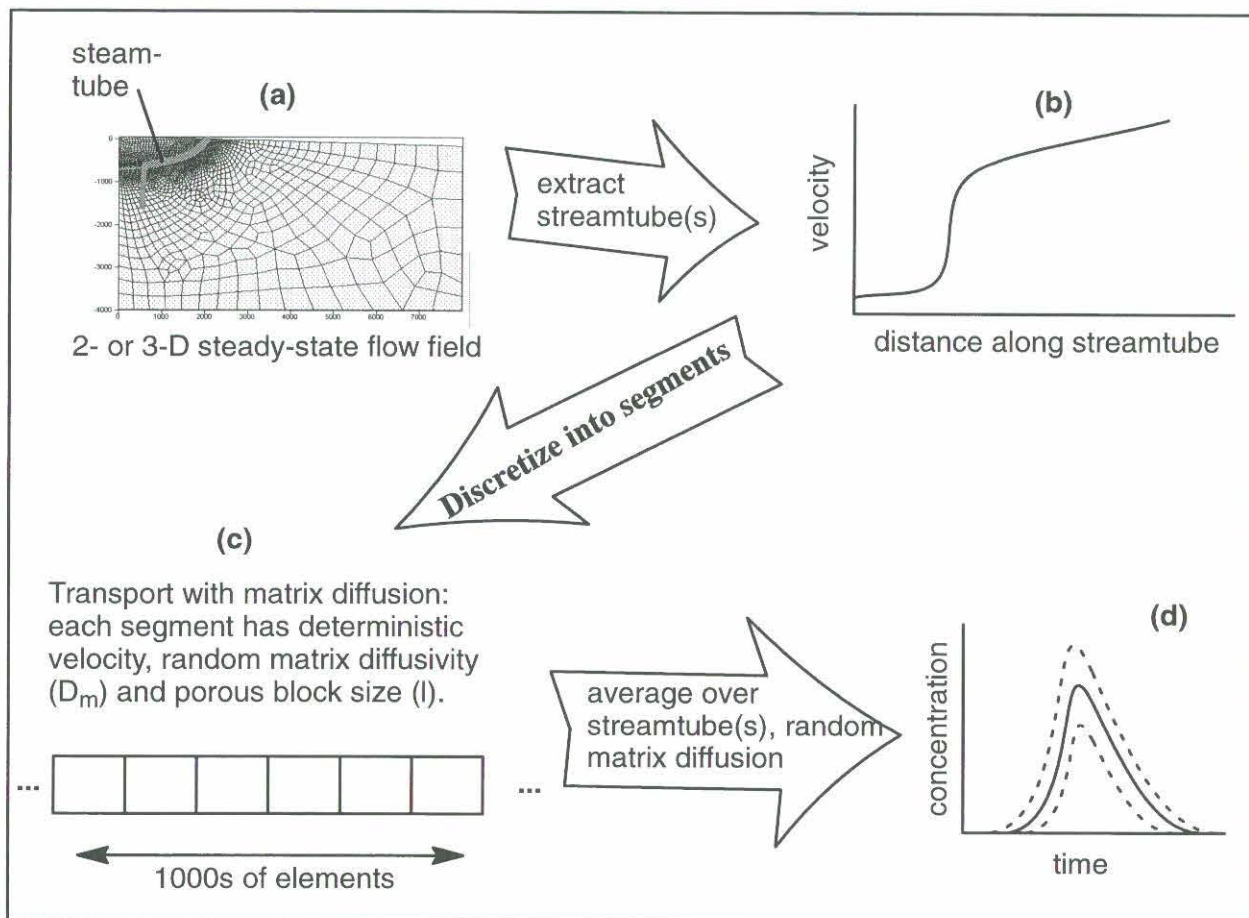


Figure 20. Schematic representation of the overall modeling effort: a) various subtasks assess the salient features that are incorporated in final flow model(s) which may be 2-D or 3-D; b) velocity data along one or more streamtubes are extracted; c) radionuclides are transported along streamtube(s) with random matrix diffusion parameters; giving d) expected and/or range of concentration breakthrough curves.

- Identify the area of ocean bottom where the highest concentrations of radionuclides are likely to enter the ocean;
- Extract velocity versus path length along one or more flowpaths from the cavity (Figure 20b);
- Simulate the random process of matrix diffusion based on measured statistical properties of the matrix diffusion parameters (Figure 20c); and
- Generate breakthrough curves based on realizations of the random matrix diffusion process (Figure 20d).

SUMMARY

The task of modeling the transport of radionuclides from the cavities beneath Amchitka Island is very different than for a typical density-invariant problem. The calculations are inherently more time and memory consuming. This has led to the proposed procedure of assessing the contribution of the various parameters to the solution independently and relative to each other. To arrive at a tractable problem, a number of the parameters must be eliminated. If several cannot reasonably be eliminated, then the problem may take on a new stature in terms of the required resources. Specifically, if the problem cannot be reduced to a steady-state flow solution, with decoupled matrix diffusion-controlled transport, then the study goes beyond the proposed scope of work. The inclusion of test-induced heat flow has the potential of producing such an outcome, based on the IACWG4 (1998) report and Rayleigh numbers that suggest mild density instability.

In the assessment of the individual parameter importance, a number of codes will be used to optimize the effort. The most suitable code in terms of efficiency is the 2-D SUTRA code coupled with the Argus GUI. It is hoped that the influence of faults in the vicinity of the tests is minimal, so that the study can reasonably stay in 2-D.

REFERENCES

- Benson, D.A., A.E. Carey and S.W. Wheatcraft, 1998. Numerical advective flux in highly variable velocity fields exemplified by saltwater intrusion. *J. Cont. Hyd.* (in press).
- Bredehoeft, J.D. and I.S. Papadopoulos, 1965. Rates of vertical groundwater movement estimated from the earth's thermal profile. *Water Resources Research*, 1(2):325-328.
- Ballance, W.C., 1972a. Hydraulic tests in hole UAe-1, Amchitka Island, Alaska. USGS-474-102.
- Ballance, W.C., 1972b. Hydraulic tests in hole UAe-6h, Amchitka Island, Alaska. USGS-474-104.
- Carr, W.J., L.M. Gard, Jr. and W.D. Quinlivan, 1966. Geologic reconnaissance of Amchitka Island, Alaska. USGS-474-42.
- Carr, W.J., W.D. Quinlivan and L.M. Gard, Jr., 1971. Geologic sketch map of Amchitka Island, in Carr, W. J. and W. D. Quinlivan, Progress Report on the Geology of Amchitka Island, Alaska. USGS-474-44.
- Claassen, H.C., 1978. Hydrologic processes and radionuclide distribution in a cavity and chimney produced by the Cannikin Nuclear explosion, Amchitka Island, Alaska. U.S. Geological Survey Professional Paper 712-D.
- Dudley, W.W., Jr., W.C. Ballance and V.M. Glanzman, 1977. Chapter 4 in M. L. Merritt and R. G. Fuller (eds.). *The Environment of Amchitka Island, Alaska*.
- Fenske, P.R., 1972. Event-related hydrology and radionuclide transport at the Cannikin site, Amchitka Island, Alaska. Desert Research Institute Report, NVO-1253-1.
- Henry, H.R., 1964. Effects of dispersion on salt encroachment in coastal aquifers, in *Sea Water in Coastal Aquifers*. U.S. Geological Survey Water Supply Paper, 1613-C, 70-84.

- International Advisory Committee, Working Group 4 (IACWG4), 1998. The radiological situation at the atolls of Mururoa and Fangataufa, Volume 4, Releases to the biosphere of radionuclides from underground nuclear weapons tests at the atolls (Interim version).
- Lee, W.H., 1968. Some physical properties of rocks in drill hole UAe-1, Amchitka Island, Alaska. USGS Technical Letter Amchitka 6-2.
- Lopez, D.L. and L. Smith, 1995. Fluid flow in fault zones: Analysis of the interplay of convective circulation and topographically driven groundwater flow. *Water Resources Research*, 31 (6), pp. 1489-1503.
- Lopez, D.L. and L. Smith, 1996. Fluid flow in fault zones: Influence of hydraulic anisotropy and heterogeneity on the fluid flow and heat transfer regime. *Water Resources Research*, 32 (10), pp. 3227-3235.
- Stallman, R.W., 1965. Notes on the use of temperature data for computing ground-water velocity: Nancy, France, 6th Assembly on Hydraulics Societe Hydrotechnique de France, Quest. 1, pp. 1-7.
- von Huene, R., W.J. Carr, D. McManua and M. Holmes, 1971. Marine geophysical study around Amchitka Island, Western Aleutian Islands, Alaska. USGS-474-74.
- Wheatcraft, S.W., 1995. Sea water intrusion model of Amchitka Island, Alaska. Desert Research Institute, Water Resources Center Publication No. 45127.